# Modelling the gluon propagator*

D. B. Leinweber[a], C. Parrinello[b†], J. I. Skullerud[a†] and A. G. Williams[a]

[a]CSSM *and* Department of Physics and Mathematical Physics,
The University of Adelaide, SA 5005, Australia

[b]Department of Mathematical Sciences, University of Liverpool,
Liverpool L69 3BX, England

Scaling of the Landau gauge gluon propagator calculated at $\beta = 6.0$ and at $\beta = 6.2$ is demonstrated. A variety of functional forms for the gluon propagator calculated on a large ($32^3 \times 64$) lattice at $\beta = 6.0$ are investigated.

## 1. SCALING BEHAVIOUR

In this note we focus on modelling the gluon propagator calculated in [1]. We use the same conventions and definitions here as in [1].

The lattice gluon propagator is related to the renormalised continuum propagator $D_R(q;\mu)$ via a renormalisation constant,

$$D^L(qa) = Z_3(\mu, a) D_R(q;\mu) \,. \tag{1}$$

The asymptotic behaviour of the renormalised gluon propagator in the continuum is given to one-loop level by

$$D_R(q) = \frac{1}{q^2}\left(\frac{1}{2}\ln(q^2/\Lambda^2)\right)^{-d_D} \tag{2}$$

with $d_D = 13/44$ in Landau gauge for quenched QCD.

Since the renormalised propagator $D_R(q;\mu)$ is independent of the lattice spacing, we can use (1) to derive a simple, $q$-independent expression for the ratio of the unrenormalised lattice gluon propagators at the same value of $q$:

$$\frac{D_c(qa_c)}{D_f(qa_f)} = \frac{Z_3(\mu, a_c) D_R(q;\mu)/a_c^2}{Z_3(\mu, a_f) D_R(q;\mu)/a_f^2} = \frac{Z_c}{Z_f}\frac{a_f^2}{a_c^2} \tag{3}$$

where the subscript $f$ denotes the finer lattice ($\beta = 6.2$ in this study) and the subscript $c$ denotes the coarser lattice ($\beta = 6.0$). We can use this relation to study directly the scaling properties of the lattice gluon propagator by matching the data for the two values of $\beta$. This matching can be performed by adjusting the values for the ratios $R_Z = Z_f/Z_c$ and $R_a = a_f/a_c$ until the two sets of data lie on the same curve. We have implemented this by making a linear interpolation of the logarithm of the data plotted against the logarithm of the momentum for both data sets. In this way the scaling of the momentum is accounted for by shifting the fine lattice data to the right by an amount $\Delta_a$ as follows

$$\ln D_c(\ln(qa_c)) = \ln D_f(\ln(qa_c) - \Delta_a) + \Delta_Z \tag{4}$$

Here $\Delta_Z$ is the amount by which the fine lattice data must be shifted up to provide the optimal overlap between the two data sets. The matching of the two data sets has been performed for values of $\Delta_a$ separated by a step size of 0.001. $\Delta_Z$ is determined for each value of $\Delta_a$ considered, and the optimal combination of shifts is identified by searching for the global minimum of the $\chi^2$/dof. The ratios $R_a$ and $R_Z$ are related to $\Delta_a$ and $\Delta_Z$ by $R_a = \exp(-\Delta_a)$; $R_Z = R_a^2 \exp(-\Delta_Z)$.

We considered matching the lattice data using $\hat{q} = 2\pi n/L$ as the momentum variable. The minimum value for $\chi^2$/dof of about 1.7 was obtained for $R_a \sim 0.815$. This value for $R_a$ is considerably higher than the value of $0.716 \pm 0.040$ obtained from an analysis of the static quark potential in [2]. From this discrepancy, as well as the relatively high value for $\chi^2$/dof, we may conclude that the gluon propagator, taken as a function of $\hat{q}$, does not exhibit scaling behaviour for the values of $\beta$ considered here.

*Talk presented by D. B. Leinweber
†UKQCD Collaboration

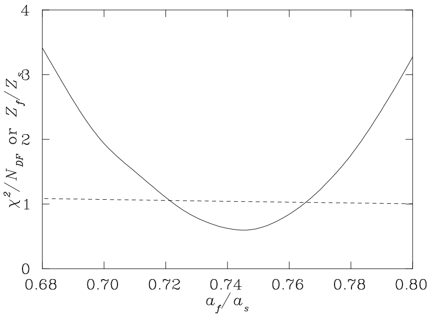


Figure 1. $\chi^2$ per degree of freedom as a function of the ratio of lattice spacings for matching the small and fine lattice data, using $q$ as the momentum variable. The dashed line indicates the ratio $R_Z$ of the renormalisation constants.

Fig. 1 shows the result of the matching using $q = 2\sin(\hat{q}/2)$ as the momentum variable. This gives much more satisfactory values both for $\chi^2$/dof and for $R_a$. The minimum value for $\chi^2$/dof of 0.6 is obtained for $R_a = 0.745$. Taking a confidence interval where $\chi^2/\text{dof} < \chi^2_{min}+1$ gives us an estimate of $R_a = 0.745^{+32}_{-37}$, which is fully compatible with the value [2] of $0.716 \pm 0.040$.

## 2. MODEL FITS

We have demonstrated scaling in our lattice data over the entire range of $q^2$ considered, and will now proceed with model fits. The following functional forms have been considered:

**Gribov [3]**

$$D_r(q^2) = \frac{q^2}{q^4 + M_{\text{IR}}^4} L(q^2, M_{\text{IR}}) \tag{5}$$

**Stingl [4]**

$$D_r(q^2) = \frac{q^2}{q^4 + 2A^2q^2 + M_{\text{IR}}^4} L(q^2, M_{\text{IR}}) \tag{6}$$

**Marenzoni [5]**

$$D_r(q^2) = \frac{1}{(q^2)^{1+\alpha} + M_{\text{IR}}^2} \tag{7}$$

**Cornwall [6]**

$$D_r(q^2) = \left[(q^2 + M^2(q^2)) \ln \frac{q^2 + 4M^2(q^2)}{\Lambda^2}\right]^{-1} \tag{8}$$

**Model A**

$$D_r(q^2) = \frac{A}{(q^2 + M_{\text{IR}}^2)^{1+\alpha}} + D_{\text{UV}}(q^2) \tag{9}$$

**Model B**

$$D_r(q^2) = \frac{A}{(q^2)^{1+\alpha} + (M_{\text{IR}}^2)^{1+\alpha}} + D_{\text{UV}}(q^2) \tag{10}$$

**Model C**

$$D_r(q^2) = Ae^{-(q^2/M_{\text{IR}}^2)^\alpha} + D_{\text{UV}}(q^2) \tag{11}$$

where $D(q^2) \equiv ZD_r(q^2)$ and

$$D_{\text{UV}}(q^2) = \frac{1}{q^2 + M_{\text{UV}}^2} L(q^2, M_{\text{UV}}) \tag{12}$$

$$L(q^2, M) = \left(\frac{1}{2}\ln((q^2 + M^2)/M^2)\right)^{-d_D} \tag{13}$$

$$M(q^2) = M\left\{\ln \frac{q^2 + 4M^2}{\Lambda^2} / \ln \frac{4M^2}{\Lambda^2}\right\}^{-6/11} \tag{14}$$

We have also considered the models A and B, which are constructed from models A and B by setting $M_{\text{UV}} = M_{\text{IR}}$. Gribov's and Stingl's models (5) and (6) are modified in order to exhibit the asymptotic behaviour of (2). Models A and B are constructed as generalisations of (7) with the correct dimension and asymptotic behaviour.

All models are fitted to the large lattice data using the cylindrical cut defined in [1,7]. The lowest momentum value was excluded, as the volume dependence of this point could not be assessed. In order to balance the sensitivity of the fit between the high- and low-momentum region, nearby data points within $\Delta(qa) < 0.05$ were averaged.

The $\chi^2$ per degree of freedom and parameter values for fits to all these models are shown in table 1. It is clear that model B accounts for the data better than any of the other models. The best fit to this model is illustrated in fig. 2.

## 3. DISCUSSION AND OUTLOOK

We have demonstrated that the gluon propagator exhibits scaling over a wide range of momenta $q$. The data are consistent with a functional form $D_r(q^2) = D_{\text{IR}} + D_{\text{UV}}$, where

$$D_{\text{IR}} = \frac{1}{2}\frac{1}{q^4 + M^4}, \tag{15}$$

Table 1
Parameter values for fits to models (5)–(11). The values quoted are for fits to the entire set of data. The errors denote the uncertainties in the last digit(s) of the parameter values which result from varying the fitting range [8].

| Model | $\chi^2$/dof | $Z$ | $A$ | $M_{\rm IR}$ | $M_{\rm UV}$ or $\Lambda$ | $\alpha$ |
|---|---|---|---|---|---|---|
| Gribov | 1972 | $2.19^{+31}_{-15}$ | | $0.23^{+14}_{-1}$ | | |
| Stingl | 1998 | 2.2 | 0 | 0.23 | | |
| Marenzoni | 163 | $2.41^{+0}_{-12}$ | | $0.14^{+4}_{-14}$ | | $0.29^{+6}_{-2}$ |
| Cornwall | 50.3 | $6.5^{+7}_{-9}$ | | $0.24^{+3}_{-16}$ | $0.27^{+7}_{-7}$ | |
| A | 2.96 | $1.54^{+10}_{-20}$ | $1.24^{+21}_{-21}$ | $0.46^{+2}_{-14}$ | $0.96^{+47}_{-17}$ | $1.31^{+16}_{-43}$ |
| A’ | 3.73 | $1.71^{+9}_{-0}$ | $0.84^{+0}_{-29}$ | $0.48^{+2}_{-17}$ | | $1.52^{+12}_{-37}$ |
| B | 1.57 | $1.78^{+45}_{-20}$ | $0.49^{+17}_{-6}$ | $0.43^{+5}_{-1}$ | $0.20^{+37}_{-19}$ | $0.95^{+7}_{-5}$ |
| B’ | 4.00 | $1.62^{+3}_{-4}$ | $0.58^{+5}_{-1}$ | $0.40^{+9}_{-2}$ | | $0.92^{+17}_{-1}$ |
| C | 47 | $2.09^{+30}_{-12}$ | $29^{+166}_{-2}$ | $0.22^{+0}_{-16}$ | $0.14^{+11}_{-10}$ | $0.49^{+0}_{-16}$ |

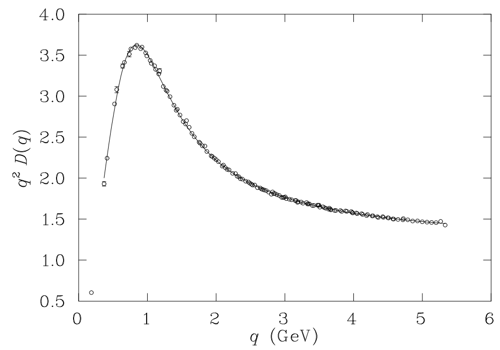


Figure 2. The gluon propagator multiplied by $q^2$, with nearby points averaged. The line illustrates our best fit to the form defined in (10). The scale is taken from the string tension [2].

$M = 0.81^{+9}_{-2}$ GeV, and $D_{\rm UV}$ is the asymptotic form given by (12) and (13). A more detailed analysis [8] of the asymptotic behaviour reveals that the one-loop formula (2) remains insufficient to describe data in the region $q^2 \sim 25{\rm GeV}^2$.

Issues for future study include the effect of Gribov copies and of dynamical fermions. We also hope to use improved actions to perform realistic simulations at larger lattice spacings. This would enable us to evaluate the gluon propagator on larger physical volumes, giving access to lower momentum values.

## ACKNOWLEDGMENTS

The numerical work was mainly performed on a Cray T3D at EPCC, University of Edinburgh, using UKQCD Collaboration time under PPARC Grant GR/K41663. Financial support from the Australian Research Council is gratefully acknowledged.

## REFERENCES

1. D.B. Leinweber, C. Parrinello, J.I. Skullerud, A.G. Williams: *The structure of the gluon propagator*, these proceedings.
2. G.S. Bali and K. Schilling, Phys. Rev. D 47, 661 (1993)
3. V.N. Gribov, Nucl. Phys. B 139, 19 (1978); D. Zwanziger, Nucl. Phys. B 378, 525 (1992)
4. M. Stingl, Phys. Rev. D 34, 3863 (1986); Phys. Rev. D 36, 651 (1987)
5. P. Marenzoni, G. Martinelli, N. Stella, Nucl. Phys. B 455, 339 (1995); P. Marenzoni *et al*, Phys. Lett. B 318, 511 (1993)
6. J. Cornwall, Phys. Rev. D 26, 1453 (1982)
7. D.B. Leinweber, J.I. Skullerud, A.G. Williams, C. Parrinello, Phys. Rev. D 58, 031501 (1998)
8. D.B. Leinweber, C. Parrinello, J.I. Skullerud, A.G. Williams, in preparation.